Vietnam Journal of Chemistry, International Edition, **55**(5): 645-651, 2017
DOI: 10.15625/2525-2321.2017-00523

Elucidating the chemical state of elements in CaO-CuO-CeO_2 mixed oxide by X-ray photoelectron spectroscopy

Pham Anh Son*, Hoang Thi Huong Hue

Faculty of Chemistry, Hanoi University of Science, VNU Hanoi

Received 14 April 2017; Accepted for publication 20 October 2017

Abstract

In this research, three-component-oxide CaO-CuO-CeO_2 was fabricated a sol-gel method. This mixed oxide acted as the catalysts for the complete oxidation of phenol in the presence of hydro peroxide. The activity of the catalyst was monitored versus fabrication conditions of mixed oxide such as aging temperature, calcination temperature and time. Under the optimum conditions including aging temperature at 70 ^oC, calcination at 600 ^oC for 30 min, the catalyst gave the best activity with 96.3% phenol conversion. Among tested mixed oxides or single oxides, three-component-oxide CaO-CuO-CeO_2 exhibited the highest performance. The chemical state of metal elements in the mixed oxide was carefully studied by high-resolution X-ray photoelectron spectroscopy (XPS) technique. The XPS spectra of Ca 2p, Cu 2p, and Ce 3d were recorded in ranges of 935-965, 927-967, and 878-930 eV, respectively. The curve fitting processes were carried out on CasaXPS version 2.3.18PR1.0 software with Shirley or Tougaard background and GL(m) line shape. Some constraints such as the FWHM, splitting energy and peak area ratio of spin-orbit interaction were introduced into the fitting process in order to achieve the highest physical meaning of the spectrum deconvolution. The fitting result proved the coexistence of Ce^{4+}, Ce^{3+}, Cu^{2+} and Cu^{+} in the component of the prepared material. The formation of Ce^{3+} and Cu^{+} from the interaction between Ce^{4+} and Cu^{2+} accompanied the appearance of oxygen vacancies in the crystal structure of CeO_2 support. That process was enhanced by the presence of calcium element. Oxygen vacancies played important role in the formation of superoxide anions that were the highly active intermediate for the phenol oxidation.

Keywords. X-ray photoelectron spectroscopy, binding energy, chemical state, CaO-CuO-CeO_2, phenol oxidation.

1. INTRODUCTION

Volatile organic compounds (VOCs), emitted from a variety of industrial processes and transportation activities, are considered as an important class of air pollutants. Catalytic oxidation is one of the most developed techniques used for the elimination of VOCs, as it requires lower temperatures than thermal oxidation. Typical catalysts for VOC oxidation are mainly noble metals, which show high activity at low temperatures, but they are costly and have low stability in the presence of chloride compounds. CuO-CeO_2 mixed metal oxide is a promising family of catalysts and has been studied by many investigators in various reactions, such as the combustion of CO and CH_4, water-gas shift reaction, reduction of NO, decomposition of H_2O_2, and wet oxidation of phenol [1]. The high activity of CuO-CeO_2 is attributed to the promoting effect of ceria due to its high oxygen storage capacity and facile Ce^{4+}/Ce^{3+} redox cycle and the strong interaction between the copper oxide and oxygen vacancies on ceria support at the interface boundary. In addition, the increase of oxygen bulk mobility of ceria-based catalysts, by introducing defective sites, seems to be effective for the promotion of oxidation reactions. It was reported that calcium-doped CeO_2 would tend to introduce defects and oxygen vacancies in the CeO_2 fluorite structure, and also could lower the energy for charge transfer from oxygen ions to cerium ions [2].

In the present work, the CaO-CuO-CeO_2 mixed oxides with a change in the mole fractions of CaO and CuO were prepared by sol-gel method. The oxidation state of elements that strongly affects the catalytic activity of prepared solid. Within the scope of this research, the chemical states of calcium, copper and cerium will be investigated carefully by X-ray photoelectron spectroscopy (XPS) technique.

2. EXPERIMENTAL

2.1. Materials

Citric acid, $Ce(NO_3)_3.6H_2O$, $Cu(NO_3)_2.3H_2O$, $Ca(NO_3)_2.4H_2O$ were purchased from Merck,

phenol, H_2O_2, $K_2Cr_2O_7$ were supplied by Sigma Aldrich, and water was distilled.

2.2. Fabrication of CaO-CuO-CeO_2 mixed oxide

The CaO-CuO-CeO_2 mixed oxides with CaO content of 2.5, 5.0, 7.5, 10, 15 mol.%, and CuO content of 5, 10, 15, 20, 25 mol.% were prepared by the citric acid sol-gel method with a slight modification [2]. Briefly, $Ce(NO_3)_3.6H_2O$, $Cu(NO_3)_2.3H_2O$ and $Ca(NO_3)_2.2H_2O$ salts were dissolved in distilled water with suitable amounts. Citric acid was added in double molar amounts to the premixed nitrate solutions of cerium, copper and calcium. The obtained solution was stirred at 70-80 °C until the color of mixture solution changed from blue to green. Once the gel formed, the temperature was elevated to 150 °C quickly, and the gel foamed with the production of nitrogen oxide vapors and burnt with sparks. A solid product was obtained after the sparks were extinguished. The as-obtained powder was calcined at 400, 500, 600 and 700 °C for 10, 30, 60, 120, 180 and 240 min in air.

2.3. Techniques for characterizing materials

The phase composition and crystal structure of prepared solids were analyzed by X-Ray Diffraction method. XRD data were collected from D8 ADVANCE Bruker diffractometer using the CuKα radiation, λ = 0.15406 nm with an X-ray generator working at 40 kV and 40 mA.

X-ray Photoelectron Spectroscopy (XPS) was measured on a Shimadzu Kratos AXISULTRA DLD spectrometer using Al target at 15 kV and 10 mA. The binding energies were calibrated with C 1s level (284.8 eV) as an internal standard reference. The binding energies of Ca 2p, Cu 2p, and Ce 3d electrons were scanned with high resolution in ranges of 935-965, 927-967, and 878-930 eV, respectively. The curve fitting processes were carried out on CasaXPS version 2.3.18PR1.0 software with Shirley or Tougaard background and GL(m) line shape.

2.4. Catalytic activity tests

The catalysts were tested for the phenol oxidation reaction in a 250 mL batch reactor equipped with a thermocouple. The experiments were performed at 70 ^oC under atmospheric pressure with stirring rate of 600 rpm for 45 min. In a typical run, 0.025 g of catalyst powder was added to 150 mL of 536 mg L^{-1} phenol aqueous solution. When the reaction temperature reached 70 ^oC, 3.5 mL of 30 wt.% hydrogen peroxide were charged into the reactor and the reaction started. Complementary experiments were performed by varying the reaction conditions. During the reaction, liquid samples were taken at different time intervals and analyzed. Phenol concentrations were measured by chemical oxygen demand (COD) that was determined by colorimetric method after reflux with $K_2Cr_2O_7$ [3]. Phenol conversion was calculated by following formula:

$$\text{Conv.} = \frac{\text{COD}_{\text{initial}} - \text{COD}_{\text{final}}}{\text{COD}_{\text{initial}}} \times 100\ (\%)$$

3. RESULTS AND DISCUSSION

A series of CaO-CuO-CeO_2 were fabricated in which the CuO content was varied from 5 to 25 mol.% while the concentration of CaO was fixed at 5 mol.%. The second series of mixed oxide was prepared when fixing CuO at 15 mol.% and varying CaO concentration from 2.5 to 15 mol.%. The other conditions were kept as follows: gel aging temperature of 80 ^oC, calcination temperature and time of 500 ^oC and 60 min, respectively.

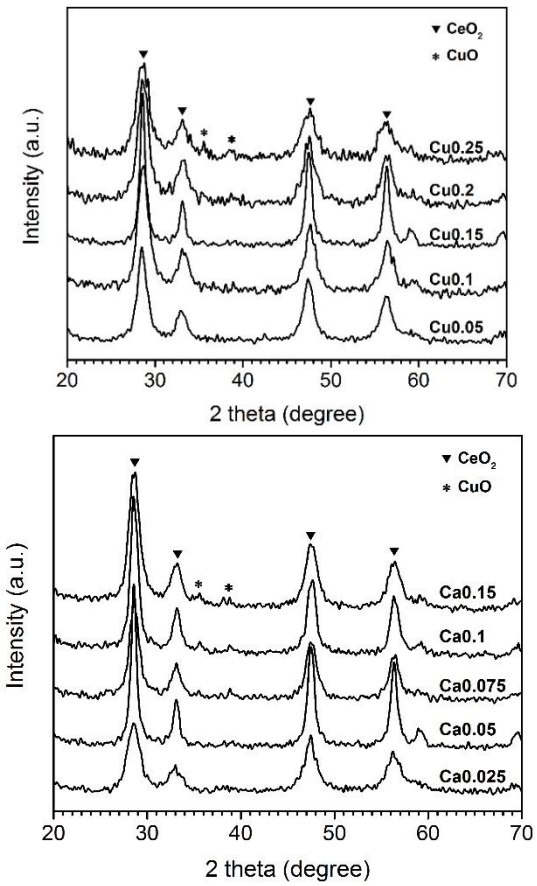

Figure 1: XRD patterns of CaO-CuO-CeO_2 mixed oxides with various CuO and CaO contents. *Fabrication conditions*: citric acid (2 times molar amount to the Ce+Cu+Ca), aging temp. (70 ^oC), calcination temp. (600 ^oC), calcination time (30 min)

On XRD patterns of all materials of the first series, there were 4 distinguishable diffraction peaks at 2θ of 28.61°, 33.26°, 47.61° and 56.45° that were characteristics of fluorite structure of CeO_2.

Table 1L The effect of CuO and CaO contents on the phase composition and catalytic activity of mixed oxides

Entry	Changed element	Content (mol.%)	Phase composition	COD_{final}	Phenol conv. (%)
1	Cu	5.0	CeO_2 (cubic)	275	80.6
2	Cu	10.0	CeO_2 (cubic)	249	82.5
3	Cu	15.0	CeO_2 (cubic)	183	87.1
4	Cu	20.0	CeO_2 (cubic) CuO (monoclinic)	220	84.5
5	Cu	25.0	CeO_2 (cubic) CuO (monoclinic)	281	80.2
6	Ca	2.5	CeO_2 (cubic)	276	80.6
7	Ca	5.0	CeO_2 (cubic)	183	87.1
8	Ca	7.5	CeO_2 (cubic)	142	90.0
9	Ca	10.0	CeO_2 (cubic) CuO (monoclinic)	203	85.7
10	Ca	15.0	CeO_2 (cubic) CuO (monoclinic)	235	83.5

Reaction conditions: catalyst (0.025 g), phenol solution (150 mL with $COD_{initial}$ = 1420 mg(O_2) L^{-1}), temperature (70 °C), 30 wt.% H_2O_2 (3.5 mL), time (45 min). 5 mol.% CaO for entries 1-5, 15 mol.% CuO for entries 6-10.

However, on XRD patterns of solids containing 20 and 25 mol.% CuO, there were other weak peaks at 35.7° and 38.8°. These peaks belonged to CuO phase with monoclinic structure. It means that copper may exist in solids in various forms. At low concentration of CuO, all added Cu atoms could replace Ce ions in the crystal lattice producing solid solution [4-5]. When the amount of CuO exceeded 15 mol.%, the individual CuO phase began to appear in samples. Similar to the first series, the main phase of all solids in second series was CeO_2 and the individual CuO phase appeared once the concentration of CaO exceeded 7.5 mol.%. Although the content of CuO in second series was kept at 15 mol.%, the monoclinic CuO phase still appeared in solids (entries 9-10) because the presence of CaO lowered the solubility of CuO in CeO_2 substrate of solid solution. It meant that the solubility of CuO was inversely related to CaO concentration [2].

The estimation of the effect of CuO and CaO contents on the catalytic activity of prepared materials can be seen in Table 1. It is easy to recognize that in each series, the increase in concentration of changed metal led the increase of phenol conversion (entries 1-3 and entries 6-8). The used solids in those experiments contained only one phase of CeO_2. The continuing rise of CuO or CaO content lowered the phenol conversion (entries 4-5 and entries 9-10). The continuing increase in these metal contents also caused the appearance of monoclinic CuO phase. Consequently, the presence of CuO phase in solids was blamed for the decline in their catalytic activity and within defined ranges of CuO and CaO concentrations, phenol conversion was found to be directly related to the content of CuO or CaO.

At low concentration, a part of copper ions could exist in the sample as amorphous CuO form, and the other parts might replace Ce^{4+} in the crystal lattice of CeO_2 to produce a solid solution. Because of the difference of positive charge between cooper and cerium ions, some oxygen ions O^{2-} must go out in order to preserve electroneutrality of solid. That process led to form the vacancies in solid solution. In these cases, the characteristic peaks of CuO were not observed in the XRD patterns. If the added amounts of modifying oxides were large enough (above 15 mol.% for CuO, and 7.5 mol.% for CaO), the CuO would appear as the contamination phase leading the decrease in phenol conversion (entries 4, 5, 9, 10) [6-8]. From above results, the appropriate contents of CuO and CaO in mixed oxides for getting maximum phenol conversion should be 15 and 7.5 mol.%, respectively. That composition prevented the formation of individual CuO phase while generated maximum quantity of oxygen vacancy in the crystal lattice [9-10], consequently, made the best catalytic activity of solid (entry 8).

At 7.5 mol.% CaO and 15 mol.% CuO, other fabrication conditions of CaO-CuO-CeO_2 solid such as aging temperature, calcination temperature and time were investigated to get the highest performance catalyst. It was found that the highest phenol conversion of 96.3% was achieved when aging precursors of CaO-CuO-CeO_2 mixed oxide at 70 °C followed by a calcination at 600 °C for 30 min.

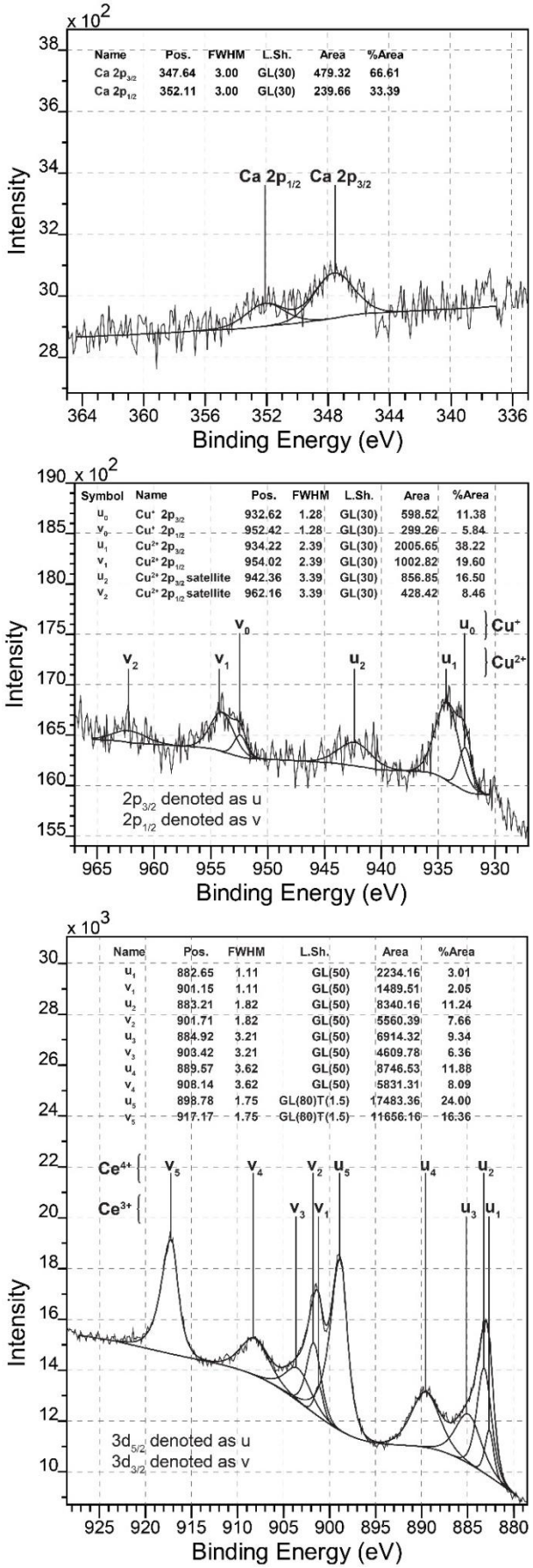

Figure 2: High resolution X-ray photoelectron spectra of Ca 2p, Cu 2p, and Ce 3d electrons

In order to estimate the preeminent property of three-component oxide of CaO-CuO-CeO_2, its catalytic activity was compared to those of other two- or one-component oxides under same reaction conditions. The phenol conversions over CeO_2, CuO, CaO-CeO_2, and CuO-CeO_2 catalysts were 14.4, 16.8, 37.2 and 61.6 %, respectively, that were much lower compared to the activity of CaO-CuO-CeO_2.

The very high activity of three-component oxide confirmed the important role of CuO for significantly improving the activity of CeO_2 as well as the positive impact of the CaO doping to the CuO-CeO_2 mixed oxide. The phenol conversion over CaO-CuO-CeO_2 catalyst increased 1.5 times compared to using CuO-CeO_2. The role of CaO doping was the increase in the concentration of oxygen vacancy in crystal lattice of CeO_2 [2, 11]. Because of its limitation, the XRD technique was not adequate to explain the all states of elements in samples. To elucidate the existence chemical states of copper and cerium species in mixed oxides, XPS technique was utilized.

In the XPS spectrum, there were weak signal from 344-356 eV that confirm the appearance of calcium element in solid. The XPS spectrum of calcium was fitted using a Shirley background type with cross section parameter of (299, 542, 275, 9.3) and peak model or line shape of GL(30). Two components were generated with the binding energy (B.E.) of 347.64 and 362.11 eV and the area ratio of 2:1. These B.E. values well agree with the references in the NIST X-Ray Photoelectron Spectroscopy Database [12]. These components were Ca $2p_{3/2}$ and Ca $2p_{1/2}$ that belong to the +2 oxidation state of calcium.

The Offset Shirley background with cross section (0.1, 0, -0.1, 0) was used for Cu 2p region. In the mixed oxide, copper might exist in both states of +1 and +2. In order to make the fitting results to have full physical meaning, some constraints were set as follows: (i) the B.E. offset between Cu $2p_{3/2}$ and Cu $2p_{1/2}$ (or spin-orbit splitting energy) was 19.8 eV [12]; (ii) the ratio of the peak areas was 2:1 (Cu $2p_{3/2}$/Cu $2p_{1/2}$); (iii) two components in each pair had same FWHM values. The curve fitting generated six individual peaks belonging to three sets denoted as (u_0,v_0), (u_1,v_1) and (u_2,v_2). In which, u represented for $2p_{3/2}$, while v was employed for $2p_{1/2}$. The fitting data was shown in Table 2. The u_0, v_0 peaks were attributed to Cu^+; while u_1, v_1, u_2, v_2 are characteristics of Cu^{2+}. In which u_1, v_1 are the main peaks; u_2, v_2 are satellite peaks resulted from shake-up process. In fact, the strong satellite peaks are only observed from bivalent copper species, while XPS

spectrum of monovalent copper species does not have or has very weak satellite peaks. The origin of satellite peaks is the charge transfer from oxygen atoms (denoted as L) to the 3d band of bivalent copper ions during the photoelectron excitation (c^{-1} term represents the core hole):

$$c^{-1}3d^{9}L \rightarrow c^{-1}3d^{10}L^{-1}$$

The charge transfer process does not occur when exciting the emission of photoelectron from monovalent coppers because Cu^{+} ions have a full 3d shell.

The concentration of each state could be calculated from its contribution to the area of main peak 2p [13]. The relative fraction of Cu^{+} was:

$$\%Cu^{+} = \frac{u_0}{u_0 + u_1} = 22.9\%$$

and therefore, Cu^{2+} fraction was 77.1 %.

Table 2: Curve fitting data of Cu 2p region

Sym.	State	B.E.	FWHM	Area	%Area
u_0	Cu^{+} $2p_{3/2}$	932.62	1.28	598.52	11.38
v_0	Cu^{+} $2p_{1/2}$	952.42	1.28	299.26	5.84
u_1	Cu^{2+} $2p_{3/2}$	934.22	2.39	2005.6	38.22
v_1	Cu^{2+} $2p_{1/2}$	954.02	2.39	1002.8	19.6
u_2	Cu^{2+} $2p_{3/2}$ sat.	942.36	3.39	856.85	16.5
v_2	Cu^{2+} $2p_{1/2}$ sat.	962.16	3.39	428.42	8.46

In the case of cerium, the satellite peaks did not appear, but the B.E. bands underwent the effect of multiplet splitting that caused the separation of each main peak into several components. The obtained main peak seemed to be asymmetric demonstrating the coexistence of both +3 and +4 oxidation states of cerium element in mixed oxide material. The curve fitting for Ce 3d region was much more complicated. The background was constructed by using Spline Tougaard model with cross section (1100, 1800, 1100, 1500). All components were fitted with GL(50) line shape, excepted the last pair peaks. For this pair, we used the GL(80)T(1.5) to obtain the best match between the calculated and experimental lines. To ensure proper peak fitting, some constrains should be considered as follows: (i) the B.E. offset between $3d_{5/2}$ and $3d_{3/2}$ (or spin-orbit splitting energy) was 18.5 eV [12]; (ii) the ratio of the peak areas was 3:2 (Ce $3d_{5/2}$/Ce $3d_{3/2}$); (iii) two components in each pair had same FWHM values and same line shape model. As shown in the Fig. 2, the Ce 3d spectrum could be fitted with 5 sets of spin-orbit doublets of Ce 3d ($3d_{5/2}$ and $3d_{3/2}$). The detail information about these 10 peaks could be found in the Table 3, in which u and v represented for $3d_{5/2}$ and $3d_{3/2}$, respectively.

Table 3: Curve fitting information of Ce 3d region

Sym.	State	B.E.	FWHM	Area	%Area
u_1	Ce^{3+} $3d_{5/2}$	882.65	1.11	2234.16	3.01
v_1	Ce^{3+} $3d_{3/2}$	901.15	1.11	1489.51	2.05
u_2	Ce^{4+} $3d_{5/2}$	883.21	1.82	8340.16	11.24
v_2	Ce^{4+} $3d_{3/2}$	901.71	1.82	5560.39	7.66
u_3	Ce^{3+} $3d_{5/2}$	884.92	3.21	6914.32	9.34
v_3	Ce^{3+} $3d_{3/2}$	903.42	3.21	4609.78	6.36
u_4	Ce^{4+} $3d_{5/2}$	889.57	3.62	8746.53	11.88
v_4	Ce^{4+} $3d_{3/2}$	908.14	3.62	5831.31	8.09
u_5	Ce^{4+} $3d_{5/2}$	898.78	1.75	17483.4	24
v_5	Ce^{4+} $3d_{3/2}$	917.17	1.75	11656.2	16.36

Three sets of spin-orbit split doublets comprising (v_2,u_2), (v_4,u_4), and (v_5,u_5) represented $3d^{10}4f^{0}$ initial electronic state that were assigned to Ce^{4+}, while Ce^{3+} with the electronic configuration of $3d^{10}4f^{1}$ contributed the appearance of the signals (v_1,u_1) and (v_3,u_3). The fraction of Ce^{4+} in the sample could be calculated from the ratio of the sum of the integrated areas of the XPS 3d peaks related to Ce^{4+} to the total integral area for the whole Ce 3d region [14-15]. Ce^{3+} fraction was:

$$\%Ce^{3+} = \frac{u_1 + v_1 + u_3 + v_3}{\sum_{i=1}^{5} u_i + v_i} = 20.7\%$$

At 15 mol.% copper and 7.5 mol.% calcium, the XRD did not show the crystalline form of CuO. Therefore, copper might exist in CaO-CuO-CeO_2 mixed oxide in two forms: amorphous CuO, and copper ions in the crystal lattice of the solid solution $Ce_{1-x-y}Ca_xCu_yO_{2-\delta}$. These two types of copper strongly interact with CeO_2 to form oxygen vacancies located on the surface as well as inside the CeO_2 lattice [16-17]. The amorphous form well dispersed on the surface of CeO_2 support. The interaction between CuO amorphous and CeO_2 on the interface yielded Ce^{3+}, Cu^{+} and the oxygen vacancies (symbolled as open square in following equation) [18]:

$$Ce^{4+} + Cu^{2+} + O^{2-} \leftrightarrow Ce^{3+} — \square — Cu^{+} + 0.5O_2\uparrow$$

These vacancies played important role in the catalytic activity of mixed oxide. The solid solution

$Ce_{1-x}Cu_xO_{2-\delta}$ was formed because of the subtitution of Ce^{4+} by Cu^{2+} ions in the crystal lattice of CeO_2. The replacement of a higher charge cation by a lower chagre one also generated the oxygen vacancies [19]:

$$Ce^{4+} + O^{2-} \leftrightarrow Cu^{2+} + \square + 0.5O_2\uparrow$$

This process was enhanced significantly when calcium element was dopped into the CuO-CeO_2 mixture. Oxygen vacancies were the sites that supplied the active oxygen in superoxide form (O_2^- anions). The O_2^- form was the result of the combination between oxygen gas and the oxygen vacancies. Superoxide form is the very active intermediate for the complete oxidation of phenol because the electrons transfer process between oxygen vacancies and the reactants could take place much easier than directly between reductants and oxidants.

4. CONCLUSION

Three-component-oxide CaO-CuO-CeO_2 was successfully fabricated via the sol-gel method. XRD result showed the single phase of CeO_2 when the contents of Cu and Ca was kept below 15 and 7.5 mol.%, respectively. The material fabricated at aging temperature of 70 ^oC, calcination at 600 ^oC for 30 min possessed the highest phenol conversion (96.3 %) that was much higher than those of other two- or one-component-oxides. The XPS results proved the coexistence of Ce(IV), Ce(III), Cu(II) and Cu(I) in the composition of solid. The formation of Ce^{3+} and Cu^+ from the interaction between Ce^{4+} and Cu^{2+} accompanied the appearance of oxygen vacancies in the crystal structure of CeO_2 support. That process was enhanced by the present of calcium element. Oxygen vacancies played important role in the formation of superoxide anions that were the highly active intermediate for the phenol oxidation.

REFERENCES

1. D. Delimaris and T. Ioannides. *VOC Oxidation over CuO-CeO_2 Catalysts Prepared by a Combustion Method*, Appl. Catal. B, **89**, 295-302 (2009).
2. D. Qiao, G. Lu, D. Mao, X. Liu, H. Li, Y. Guo and Y. Guo. *Effect of Ca Doping on the Catalytic Performance of CuO-CeO_2 Catalysts for Methane Combustion*, Catal. Commun., **11**, 858-861 (2010).
3. L. S. Clesceri, A. Geenberg, *Standard Method for the Examination of Water and Wastewater*, 20th Ed., American Public Health Association, Washington DC (1998).
4. Y. Liu, Q. Fu, M. F. Stephanopoulos. *Preferential Oxidation of CO in H_2 over CuO-CeO_2 Catalysts*, Catal. Today, **93-95**, 241-246 (2004).
5. J. Astudillo, G. Águila, F. Díaz, S. Guerrero and P. Araya, *Study of CuO-CeO_2 Catalysts Supported on SiO_2 on the Low-temperature Oxidation of CO*, Appl. Catal. A, **381**, 169-176 (2010).
6. N. F. P. Ribeiro, M. M. V. M. Souza and M. Schmal. *Combustion Synthesis of Copper Catalysts for Selective CO Oxidation*, J. Power Sources, **179**, 329-334 (2008).
7. P. Massa, F. Ivorra, P. Haure and R. Fenoglio. *Catalytic Set Peroxide Oxidation of Phenol Solutions over CuO/CeO_2 Systems*, J. Hazard Mater., **190**, 1068-1073 (2011).
8. X. C. Zheng, S. P. Wang, S. R. Wang, S. M. Zhang, W. P. Huang and S.H. Wu. *Preparation, Characterization and Catalytic Properties of CuO/CeO_2 System*, Mater. Sci. Eng. C, **25**, 516-520 (2005).
9. C. Hu. *Enhanced Catalytic Activity and Stability of $Cu_{0.13}Ce_{0.87}O_y$ Catalyst for Acetone Combustion: Effect of Calcination Temperature*, Chem. Eng. J., **159**, 129-137 (2010).
10. M. Fu, X. Yue, D. Ye, J. Ouyang, B. Huang, J. Wu and H. Liang. *Soot Oxidation via CuO Doped CeO_2 Catalysts Prepared Using Coprecipitation and Citrate Acid Complex-ombustion Synthesis*, Catal. Today, **153**, 125-132 (2010).
11. J. A. Rodriguez, X. Wang, J. C. Hanson, G. Liu, A. Iglesias-Juez and M. Fernández-García. *The Behavior of Mixed-metal Oxides: Structural and Electronic Properties of $Ce_{1-x}Ca_xO_2Ce_{1-x}Ca_xO_2$ and $Ce_{1-x}Ca_xO_{2-x}$*, J. Chem. Phys., **119**, 5659-5669 (2003).
12. *NIST X-Ray Photoelectron Spectroscopy Database*: https://srdata.nist.gov/xps/Default.aspx. Accessed date: April 4th, 2017.
13. C. M. Chanquía, K. Sapag, E. Rodríguez-Castellón, E. R. Herrero, G.A. Eimer. *Nature and Location of Copper Nanospecies in Mesoporous Molecular Sieves*, J. Phys. Chem. C, **114**, 1481-1490 (2010).
14. Y. Zhou, J. M. Perket and J. Zhou. *Growth of Pt Nanoparticles on Reducible CeO_2(111) Thin Films: Effect of Nanostructures and Redox Properties of Ceria*, J. Phys. Chem. C, **114**, 11853-11860 (2010).
15. A.S. Dieza, M. Graziano-Mayera, G. Radivoya, M. A. Volpeb. *Suzuki–Miyaura Cross-coupling of Aryl Iodides and Phenylboronic Acid over Palladium-free CeO_2 Catalysts*, Appl. Catal. A, **482**, 24-30 (2014).
16. Z. Liu, R. Zhou and X. Zheng. *Comparative Study of Different Methods of Preparing CuO-CeO_2 Catalysts for Preferential Oxidation of CO in Excess Hydrogen*, J. Mol. Catal., A: Chem., **267**, 137-142 (2007).
17. M .F. Luo, Y. P. Song, J. Q. Lu, X. Y. Wang and Z.

Y. Pu. *Identification of CuO Species in High Surface Area CuO-CeO_2 Catalysts and Their Catalytic Activities for CO Oxidation*, J. Phys. Chem., C, **111**, 12686-12692 (2007).

18. R. Zhang, T. Haddadin, D. P. Rubiano, H. Nair, C. S. Polster and C.D. Baertsch. *Quantification of Reactive CO and H_2 on CuO_x-CeO_2 During CO Preferential Oxidation by Reactive Titration and Steady State Isotopic Transient Kinetic Analysis*, ACS Catal., **1**, 519-525 (2011).
19. Q. Liang, X. Wu, D. Weng and Z. Lu. *Selective Oxidation of Soot over Cu Doped Ceria/Ceria–Zirconia Catalysts*, Catal. Commun., **9**, 202-206 (2008).

Corresponding author: **Pham Anh Son**
Department of Inorganic Chemistry
Faculty of Chemistry, Hanoi University of Science, VNU Hanoi
No. 19, Le Thanh Tong, Hoan Kiem, Hanoi
E-mail: anhsonhhvc@gmail.com.